

Structure-constrained relative acoustic impedance using stratigraphic coordinates^a

^aPublished in Geophysics, 80, no. 3, A63-A67 (2015)

Parvaneh Karimi

ABSTRACT

Acoustic impedance inversion involves conversion of seismic traces to a reflection coefficient time series, and then into acoustic impedance. The usual assumption for the transformation of post-stack seismic data into impedance, is that seismic traces can be modeled using the simple convolutional model. According to the convolutional model, a seismic trace is a normal-incidence record, which is an assumption that is strictly true only if the earth structure is composed of horizontal layers. In the presence of dipping layers, such an assumption is violated, which introduces bias in the result of impedance inversion. I propose to implement impedance inversion in the stratigraphic coordinate system, where the vertical direction is normal to reflectors and seismic traces represent normal-incidence seismograms. Tests on field data produce more accurate and detailed impedance results from inversion in the stratigraphic coordinate system, compared to impedance results using the conventional Cartesian coordinate system.

INTRODUCTION

Acoustic impedance inversion involves conversion of seismic traces to a reflection coefficient time series, and then into acoustic impedance (Lavergne and Willim, 1977; Lindseth, 1979). These impedance traces can enhance accuracy of interpretation and correlation with properties measured in well logs. Duboz et al. (1998) and Latimer and Riel (2000), among others, point out the advantages of impedance data over conventional seismic: acoustic impedance is a rock property and a product of velocity and density, both of which can be measured at well locations. Seismic reflection, in contrast, is an interface property and a relative measurement of changes in acoustic impedance between layers. Therefore having the data in layers, rather than at interfaces, improves visualization, including both layering and vertical resolution. In addition, the elimination of wavelet side-lobes and false stratigraphic-like effects makes sequence-stratigraphic analysis easier. Acoustic impedance has been shown to be correlated with lithology (Pendrel and van Riel, 1997), porosity (Brown, 1996; Burge and Neff, 1998), and other fundamental rock properties.

Although seismic-derived acoustic impedance is a powerful tool in many aspects mentioned above, it is trace-based, which can cause errors in the presence of dipping layers. According to the convolutional model, seismic traces are considered normal-incidence 1D seismograms, which is strictly true only in the case of horizontal layers. When the subsurface exhibits dipping layers, the convolutional model will no longer hold true, because the seismic waveform will be sampled vertically instead of normally to the reflector (Guo and Marfurt, 2010), introducing a possible bias in the acoustic-impedance result.

In this paper, I propose to approach this problem and improve the accuracy of impedance estimates by employing the stratigraphic coordinate system (Karimi and Fomel, 2011, 2014) for impedance inversion. In stratigraphic coordinates, the vertical direction stays normal to reflectors (Mallet, 2014), conforming to the assumption of the convolutional model.

In the following sections, I start by briefly reviewing the algorithm used to generate stratigraphic coordinates. Then, I explain the proposed methodology for impedance inversion. I use a field-data example to test the proposed approach and to verify that, in the presence of dipping layers, seismic-derived impedance becomes biased and can be improved significantly by the use of stratigraphic coordinates.

METHOD

Inversion of post-stack seismic data into acoustic impedance is a classic trace-based process (Russell and Hampson, 1991). The usual assumption behind post-stack inversion methods is that a seismic trace in a stacked section satisfies the convolutional equation, which can be written as

$$s_t = r_t * w_t, \quad (1)$$

where s_t is the seismic trace, r_t is the earth's normal incidence reflectivity, and w_t is the seismic wavelet. According to equation 1, by deconvolving the seismic wavelet, one can acquire the earth's normal incidence reflectivity, which, in turn, is related to acoustic impedance through the recursive equation (Lindseth, 1979)

$$Z_{t+1} = Z_t \left[\frac{1 + r_t}{1 - r_t} \right]. \quad (2)$$

In practice, when the subsurface shows dipping layers, the convolutional model no longer holds true. Neither will the equation that relates earth's normal-incidence reflectivity to acoustic impedance (equation 2), because seismic traces in this case cannot be considered as simple 1D normal-incidence seismograms. In order to improve the accuracy of seismic-derived acoustic impedance, I propose to employ the stratigraphic coordinate system (Karimi and Fomel, 2011, 2014), in which the convolutional model assumption is more accurate.

Stratigraphic coordinates

In order to define the first step for transformation to stratigraphic coordinates, I follow the predictive-painting algorithm (Fomel, 2010), which is based on the method of plane-wave destruction for measuring local slopes of seismic events (Claerbout, 1992; Fomel, 2002). By writing plane-wave destruction in the linear operator notation as:

$$\mathbf{r} = \mathbf{D} \mathbf{s} , \quad (3)$$

where, \mathbf{s} is a seismic section ($\mathbf{s} = [\mathbf{s}_1 \ \mathbf{s}_2 \ \dots \ \mathbf{s}_N]^T$), \mathbf{r} is the destruction residual, and \mathbf{D} , the non-stationary plane-wave destruction operator, is

$$\mathbf{D} = \begin{bmatrix} \mathbf{I} & 0 & 0 & \dots & 0 \\ -\mathbf{P}_{1,2} & \mathbf{I} & 0 & \dots & 0 \\ 0 & -\mathbf{P}_{2,3} & \mathbf{I} & \dots & 0 \\ \dots & \dots & \dots & \dots & \dots \\ 0 & 0 & \dots & -\mathbf{P}_{N-1,N} & \mathbf{I} \end{bmatrix} , \quad (4)$$

where \mathbf{I} is the identity operator and $\mathbf{P}_{i,j}$ is the prediction of trace j from trace i determined by being shifted along the local slopes of seismic events. Local slopes are estimated by minimizing the destruction residual using a regularized least-squares optimization. The prediction of trace \mathbf{s}_k from a distant reference trace \mathbf{s}_r is $\mathbf{P}_{r,k} \mathbf{s}_r$, where

$$\mathbf{P}_{r,k} = \mathbf{P}_{k-1,k} \cdots \mathbf{P}_{r+1,r+2} \mathbf{P}_{r,r+1} . \quad (5)$$

This is a simple recursion, and $\mathbf{P}_{r,k}$ is called the predictive painting operator (Fomel, 2010). Predictive painting spreads the time values along a reference trace in order to output the *relative geologic age* attribute ($Z_0(x, y, z)$). These painted horizons outputted by predictive painting are used as the first axis of the stratigraphic coordinate system. In the next step, following Karimi and Fomel (2011, 2014), I find the two other axes, $X_0(x, y, z)$ and $Y_0(x, y, z)$, orthogonal to the first axis, $Z_0(x, y, z)$, by numerically solving the following gradient equations:

$$\nabla Z_0 \cdot \nabla X_0 = 0 \quad (6)$$

and

$$\nabla Z_0 \cdot \nabla Y_0 = 0. \quad (7)$$

Equations 6 and 7 simply state that the X_0 and Y_0 axes should be perpendicular to Z_0 . The boundary condition for the first gradient equation (equation 6) is

$$X_0(x, y, 0) = x \quad (8)$$

and the boundary condition for equation 7 is

$$Y_0(x, y, 0) = y. \quad (9)$$

These two boundary conditions mean that the stratigraphic coordinate system and the regular coordinate system (x, y, z) meet at the surface ($z = 0$). Note that the

stratigraphic coordinates are designed for depth images (Mallet, 2004, 2014). When applied to time-domain images, a scaling factor with dimensions of velocity-squared is added to equations 6 and 7, because the definition of the gradient operator becomes

$$\nabla = \left(\frac{\partial}{\partial x}, \frac{\partial}{\partial y}, \frac{\partial}{\partial z} \frac{\partial z}{\partial t} \right). \quad (10)$$

EXAMPLE

I use a 3D field data volume from Heidrun Field in the Halten Terrace area, offshore Mid-Norway (Moscardelli et al., 2013) to test the proposed approach (Figure 1a). I begin by estimating local slopes of seismic events through the data volume using plane-wave destruction. After that, I apply the predictive painting algorithm to obtain the first axis of the stratigraphic coordinates. The two other axes are found by solving gradient equations 6 and 7. Figure 1b shows the image in the Cartesian coordinate system, overlain by its stratigraphic coordinates grid. Figure 1c shows the image in the stratigraphic coordinate system, where major reflectors appear nearly flat, and Figure 1d displays the image reconstruction by returning from stratigraphic coordinates to Cartesian coordinates. I use model-based inversion (Russell and Hampson, 1991; Cooke and Schneider, 1983) to extract acoustic impedance information from the seismic image. Because of the band-limited nature of seismic data, low-frequency variations are extracted from the well data, and then added back to the seismic data in order to obtain a proper broad-band result. Model-based inversion starts with a low-frequency model of P -impedance and perturbs this model until the derived synthetic section from the application of equations 1 and 2 best fits the actual seismic data. In the model-based inversion, extraction of the seismic wavelet is necessary. Figure 2 shows the extracted wavelet from the seismic image in the Cartesian coordinates, Figure 2a is the time response, and Figure 2b is the frequency response of the seismic wavelet. Figure 3 shows the extracted wavelet from the seismic image in the stratigraphic coordinate system.

Figure 4a is a zoomed-in part of the image, and Figure 4b is the impedance results obtained from inversion in the Cartesian coordinates. Figure 4c shows the impedance inversion result acquired in the stratigraphic coordinate system and transferred back to Cartesian coordinate system to provide a better comparison. Comparing the impedance acquired from inversion in the conventional Cartesian coordinates (Figures 4b) with the result obtained from inversion in the stratigraphic coordinates (Figures 4c) shows that result from inversion in stratigraphic coordinates (Figures 4c) appears to be more consistent with the geological structure and also more detailed. Interfaces are noticeably better defined and laterally more continuous. This improved accuracy result because, in the stratigraphic coordinates, layers get flattened and the vertical direction corresponds to the normal direction to reflectors, and therefore allows for a more accurate analysis of the earth's normal incidence reflectivity and its impedance.

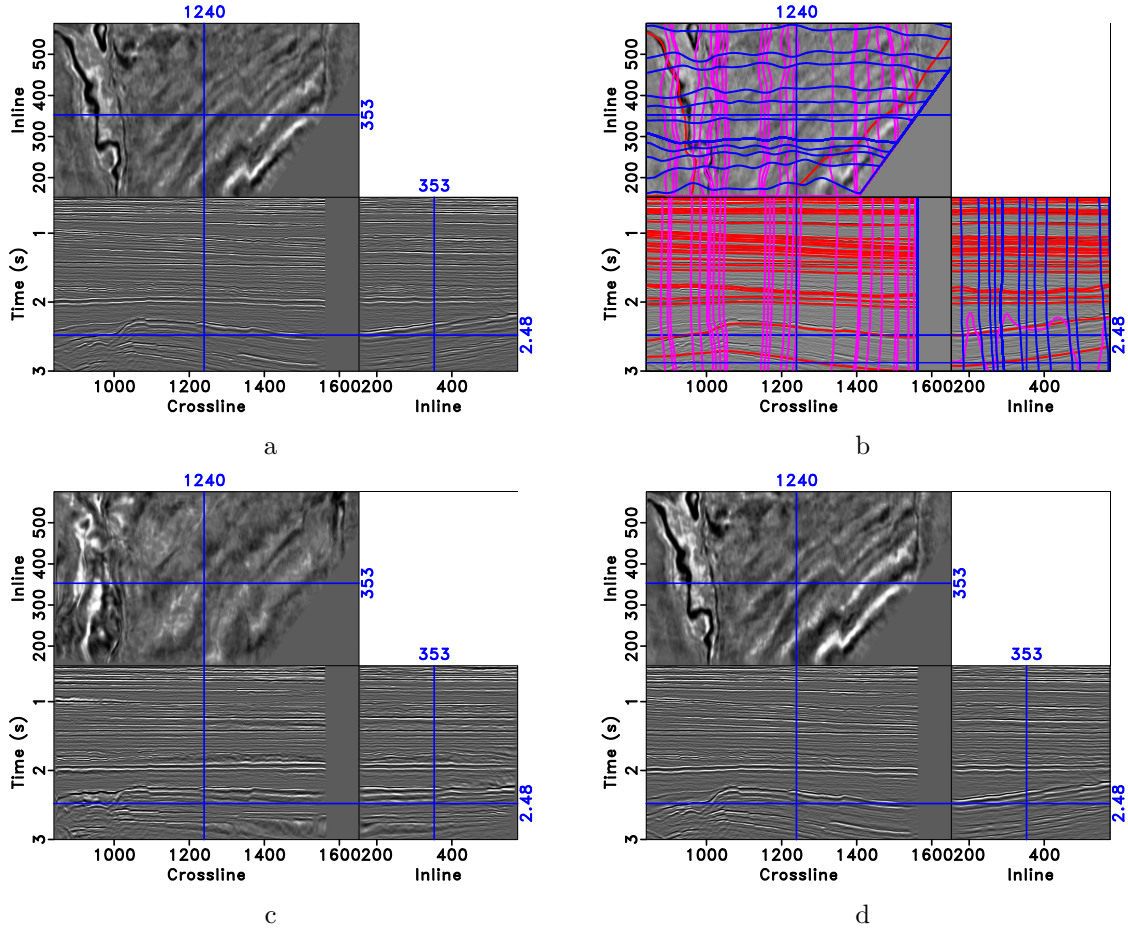


Figure 1: (a) 3D field data from Heidrun. (b) Three axes of stratigraphic coordinates of Figure 1a plotted as grid in their Cartesian coordinates. (c) Heidrun image after flattening by transferring the image to stratigraphic coordinates. (d) Heidrun image reconstruction by returning from stratigraphic coordinates to Cartesian coordinates.

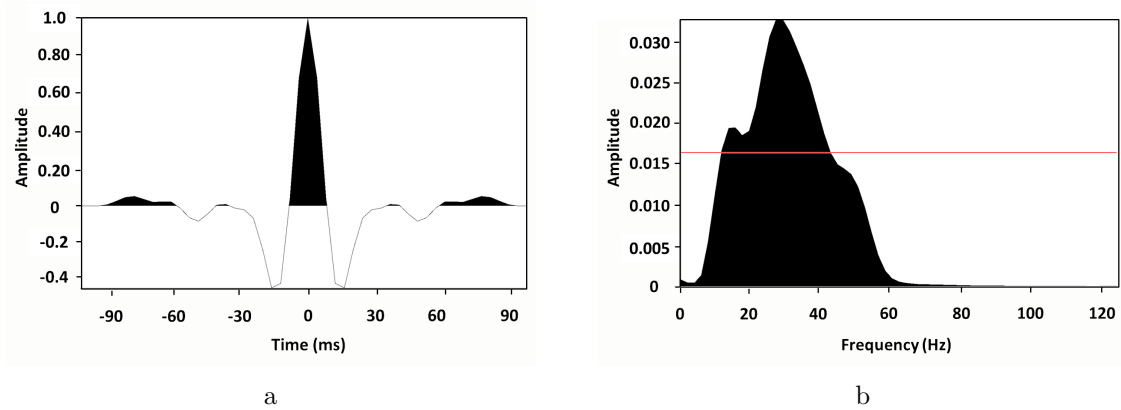


Figure 2: Extracted wavelet from the seismic data in Figure 1a in the Cartesian coordinates, (a) is the time response and (b) is the frequency response.

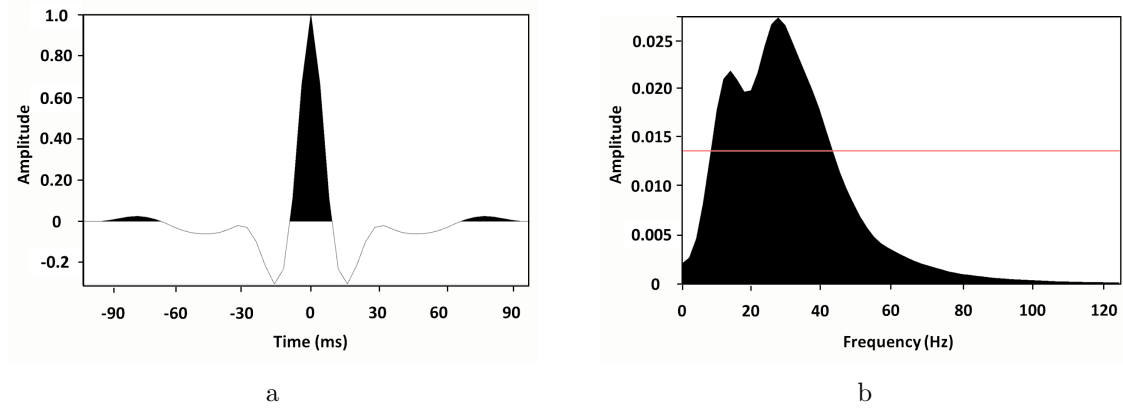


Figure 3: Extracted wavelet from the seismic data in Figure 1c in the stratigraphic coordinates, (a) is the time response and (b) is the frequency response.

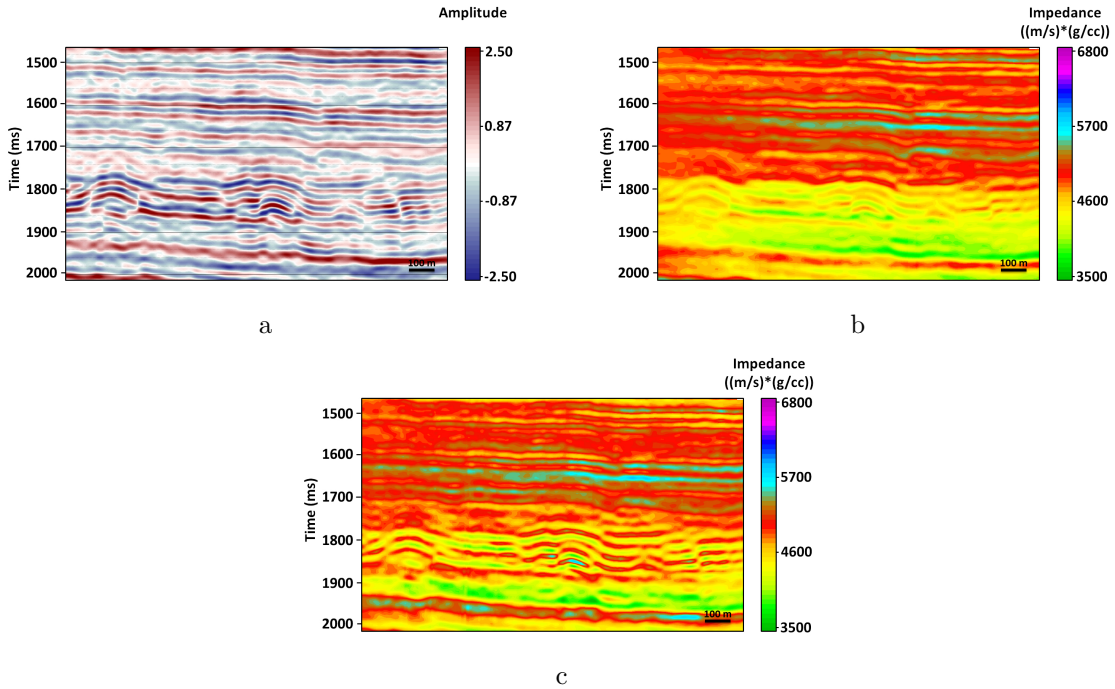


Figure 4: (a) A zoomed-in part of the Figure 1a and the impedance result obtained from inversion in the Cartesian coordinates (b), and in the stratigraphic coordinates (the result is transferred back to Cartesian coordinates to provide a better comparison) (c).

DISCUSSION AND CONCLUSIONS

Post-stack impedance inversion involves the assumption that seismic traces can be modeled using the convolutional and vertical-incidence reflection-coefficient equations. In the presence of dipping layers, these assumptions are false, and therefore seismic-derived acoustic impedance can be biased. To solve this problem, I have employed the stratigraphic coordinate system, which offers a local reference frame extracted from the seismic image and naturally designed to sample the unbiased normal incidence seismic traces, and hence yield more accurate impedance estimates.

Performance of the stratigraphic coordinate system is based on the predictive-painting algorithm, which produces the best results when seismic traces can be predicted from neighboring traces. Note that the predictive painting approach may require further improvements to deal with areas where either structural or stratigraphic discontinuities are present. Future research should concentrate on using a small number of control points especially near discontinuities interactively in the predictive painting algorithm to make sure that the events across structural or stratigraphic discontinuities are accurately captured.

ACKNOWLEDGMENTS

I thank ConocoPhillips, the Norwegian Petroleum Directorate, the Quantitative Clastics Laboratory (QCL) Industrial Associates Program, and personally Lorena Moscardelli for facilitating access to data used in this study. I would like to thank Sergey Fomel and Mehdi Far for helpful discussions. I also thank reviewers for their constructive suggestions, which helped improve this paper.

REFERENCES

- Brown, A. R., 1996, Interpretation of three-dimensional seismic data: 4th ed, AAPG Memoir 42, 424.
- Burge, D. W., and D. B. Neff, 1998, Well-based seismic lithology inversion for porosity and pay-thickness mapping: *The Leading Edge*, **17**, no. 2, 166–171.
- Claerbout, J. F., 1992, *Earth sounding analysis: Processing versus inversion*: Blackwell Science.
- Cooke, D. A., and W. A. Schneider, 1983, Generalized linear inversion of reflection seismic data: *Geophysics*, **48**, 665–676.
- Duboz, P., Y. Lafet, and D. Mougnot, 1998, Moving to a layered impedance cube: advantages of 3D stratigraphic inversion: *First Break*, **16**, no. 9, 311–318.
- Fomel, S., 2002, Applications of plane-wave destruction filters: *Geophysics*, **67**, no. 6, 1946–1960.
- , 2010, Predictive painting of 3-D seismic volumes: *Geophysics*, **75**, no. 4, A25–A30.

- Guo, H., and K. J. Marfurt, 2010, Spectral decomposition along the travel path of signal wavelets: Expanded Abstracts 80th SEG International Convention, 1478–1482.
- Karimi, P., and S. Fomel, 2011, Stratigraphic coordinate system: 81st Annual International Meeting, SEG, Expanded Abstracts.
- , 2014, Stratigraphic coordinates, a coordinate system tailored to seismic interpretation: *Geophys. Prosp.*, in press.
- Latimer, R. B., and R. D. P. V. Riel, 2000, An interpreter's guide to understanding and working with seismic-derived acoustic impedance data: *The Leading Edge*, **19**, 242–256.
- Lavergne, M., and C. Willim, 1977, Inversion of seismograms and pseudo velocity logs: *Geophysical Prospecting*, **25**, no. 2, 231–250.
- Lindseth, R. O., 1979, Synthetic sonic logs—a process for stratigraphic interpretation: *Geophysics*, **44**, no. 1, 3–26.
- Mallet, J. L., 2004, Space-time mathematical framework for sedimentary geology: *Mathematical Geology*, **36**, A25–A30.
- , 2014, Elements of mathematical sedimentary geology: the geochron model: EAGE Publications bv.
- Moscardelli, L., S. K. Ramnarine, L. Wood, and D. Dunlap, 2013, Seismic geomorphological analysis and hydrocarbon potential of the lower Cretaceous Cromer Knoll Group, Heidrun Field, Norway: *AAPG Bulletin*, **97**, no. 8, 1227–1248.
- Pendrel, J. V., and P. van Riel, 1997, Methodology for seismic inversion, a western Canadian reef example: *Canadian Society of Exploration Geophysicists Recorder*, **22**, no. 5.
- Russell, B., and D. Hampson, 1991, A comparison of post-stack seismic inversion methods: Annual Meeting Abstracts, Society of Exploration Geophysicists, 876–878.